Progress of Theoretical Physics, Vol. 103, No. 2, February 2000

Theoretical and Experimental K^++ Nucleus Total and Reaction Cross Sections from the KDP-RIA Model

L. Kurth Kerr, B. C. Clark, S. Hama,* L. Ray** and G. W. Hoffmann**

Department of Physics, The Ohio State University, Columbus, Ohio 43210-1106 USA

**Hiroshima University of Economics, Hiroshima 731-0192, Japan*

***Department of Physics, The University of Texas at Austin, Austin, Texas 78712 USA*

(Received August 12, 1999)

The 5-dimensional spin-0 form of the Kemmer-Duffin-Petiau (KDP) equation is used to calculate scattering observables [elastic differential cross sections ($d\sigma/d\Omega$), total cross sections ($\sigma_{\rm Tot}$), and total reaction cross sections ($\sigma_{\rm Reac}$)] and to deduce $\sigma_{\rm Tot}$ and $\sigma_{\rm Reac}$ from transmission data for K^++ ^{6}Li, ^{12}C, ^{28}Si and ^{40}Ca at several momenta in the range 488–714 MeV/c. Realistic uncertainties are generated for the theoretical predictions. These errors, mainly due to uncertainties associated with the elementary K^++ nucleon amplitudes, are large, which may account for some of the disagreement between experimental and theoretical $\sigma_{\rm Tot}$ and $\sigma_{\rm Reac}$. The results suggest that the K^++ nucleon amplitudes need to be much better determined before further improvement in the understanding of these data can occur.

§1. Introduction

For K^+ mesons of momenta 500 – 1000 MeV/c (laboratory), a simple first-order impulse approximation model should account for the main features of K^++ nucleus (A) scattering observables. Such expectation arises from the fact that the K^++ nucleon (K^+N) effective interaction is relatively weak, hence multiple scattering corrections to the first-order impulse approximation predictions should be relatively small.[1)] Thus it was surprising that the first 800 MeV/c elastic scattering differential cross section data[2)] for ^{12}C(K^+,K^+) and ^{40}Ca(K^+,K^+) were consistently underestimated by a number of different first-order impulse approximation calculations.[3)-5)] In addition, calculated total cross sections for $K^+ + A$ were found to be much smaller[5),6)] than experimental values.[7),8)] These findings prompted suggestions that unconventional medium effects might explain the discrepancies.[4),9)-11)]

The disagreement between the calculated elastic differential cross sections and the data of Ref. 2) does not provide firm evidence for medium effects because of the 17% absolute normalization uncertainty for the data; this alone can account for much of the discrepancy. Indeed, more recently, it was shown that 715 MeV/c elastic differential cross section data for ^{12}C(K^+,K^+) are well-described by first-order impulse approximation calculations.[12)] Yet these calculations[6)] did not fit the total cross section data for K^++^{12}C at similar energies. Friedman et al.[13)] noted, however, that the experimental total cross sections[7),8)] are, in fact, model-dependent quantities, and that it is essential to use the same $K^+ + A$ scattering model for obtaining the "experimental" total cross sections from measured transmission data as is used for calculating theoretical total cross sections. They reanalyzed data from a transmission experiment and explored the model-dependence of the deduced total ($\sigma_{\rm Tot}$) and reaction ($\sigma_{\rm Reac}$) cross sections. In spite of the fact that care was taken to conduct a self-consistent analysis of the data, the authors of Ref. 13) concluded that "there seems to remain a significant and puzzling discrepancy between theory and experiment for K^+ nuclear interactions at intermediate energies ($p_L \approx 500 - 800$ MeV/c)". One thing that has been lacking so far in these studies is an evaluation of the uncertainties in the theoretical predictions.

In this work we examine the discrepancies between the $K^+ + A$ total and reaction cross section predictions and data using the 5-dimensional spin-0 form of the relativistic Kemmer-Duffin-Petiau (KDP) equation[3)] which we use to calculate $K^+ + A$ elastic scattering observables and to deduce total and reaction cross sections from transmission data. Our emphasis is on determining whether the relativistic KDP scattering model yields predictions which are in better agreement with experiment, whether the discrepancies can in any way be due to model dependence in the experimental total and reaction cross sections, and whether some or all of the discrepancy could be due to inaccuracies in the K^+N amplitude input to the theoretical predictions.

The KDP equation, unlike the Klein-Gordon (KG) equation, is a linear equation of motion resembling the Dirac equation in form which, because of its linearity, facilitates the construction of a meson-nucleus optical potential by way of a relativistic multiple scattering approach analogous to that used to generate the nucleon-nucleus relativistic impulse approximation (RIA)[14)] optical potential. The meson-nucleus optical potential in the KDP-RIA approach consists of large and nearly cancelling scalar and vector (time-like) components which are determined by folding the elementary K^+N amplitudes[15)] with the relativistic mean-field Hartree densities of Furnstahl et al.[16)] The calculated scattering observables are thus subject to the uncertainties in the elementary amplitudes[17)] and in the nuclear densities.

The KDP-RIA model was used to calculate the $K^+ + A$ total ($\sigma_{\rm Tot}$) and reaction ($\sigma_{\rm Reac}$) cross sections for $K^+ +$ ^{6}Li, ^{12}C, ^{28}Si and ^{40}Ca at several momenta in the range 488 – 714 MeV/c; the same model was used to extract experimental $\sigma_{\rm Tot}$ and $\sigma_{\rm Reac}$ from transmission data. We also calculated the 715 MeV/c $K^+ + ^{12}$C elastic differential cross section ($d\sigma/d\Omega$) for comparison with data.

The goals of this paper are: (1) to test the KDP-RIA theoretical model by comparing the predictions with recent $K^+ + A$ scattering data, (2) to study the model dependence in the "experimental" total and reaction cross sections obtained from the transmission data, and (3) to estimate the uncertainties in the first-order impulse approximation predictions for $K^+ + A$ $\sigma_{\rm Tot}$, $\sigma_{\rm Reac}$ and the differential cross section.

The KDP-RIA model for meson-nucleus scattering is reviewed and summarized in §2. The method for obtaining total cross sections from the transmission measurements is described in §3. The numerical results and discussion are presented in §4 followed in §5 by our conclusions.

§2. The relativistic impulse approximation in the KDP formalism

In this section we discuss a treatment of meson-nucleus elastic scattering using the nucleon-nucleus Dirac RIA as a guide in developing the parameter-free optical potentials. Standard optical model treatments of meson-nucleus scattering have generally used the Klein-Gordon or Schrödinger equations as the relevant one-body wave equation. Here we review and summarize an alternative approach introduced in Ref. 3) using the first-order KDP wave equation which is similar in form to the Dirac equation. This approach is motivated by three general considerations. First, the equation is linear in energy which facilitates the development of impulse approximation optical potentials in a manner analogous to the nucleon-nucleus RIA. Second, the richness of the KDP formalism regarding the introduction of interactions is intriguing. For example, if the interaction has a conserved vector current then the KDP formalism gives identical results to the KG equation for spin zero projectiles. If the interactions do not have a conserved current or if scalar interactions are considered this is not necessarily the case.[18)] Third, the KDP equation is appropriate for both spin zero and spin one projectiles.

The free particle KDP equation is ($\hbar = c = 1$)

$$(i\beta^{\mu}\partial_{\mu} - m)\phi = 0, \tag{1}$$

where m is the mass parameter, $\mu = 0, 1, 2, 3$, and the β^{μ} obey

$$\beta^{\mu}\beta^{\nu}\beta^{\lambda} + \beta^{\lambda}\beta^{\nu}\beta^{\mu} = g^{\mu\nu}\beta^{\lambda} + g^{\lambda\nu}\beta^{\mu}. \tag{2}$$

The algebra generated by the four β^{μ}'s has three irreducible representations of dimension one, five and ten. The five dimensional representation yields a spin operator whose eigenvalues are zero, the ten dimensional case corresponds to spin one and the one dimensional case is trivial. The first component of the five dimensional Kemmer wave function for the spin zero case satisfies the Klein-Gordon equation for massive particles.

In order to apply the KDP formalism to meson-nucleus scattering we must introduce interactions in Eq. (1). If one writes

$$(i\beta^{\mu}\partial_{\mu} - m - U)\phi = 0 \tag{3}$$

the most general form for U contains two scalar, two vector and two tensor terms.[19)] We omit the tensors to avoid noncausal effects.[19)] For the spin zero case the scalar operators are the unit operator I and the 5×5 operator P whose elements are all zeros except the (1,1) element; thus P acts as a projection operator onto the first component of ϕ. The vector operators are β^{μ} and $\tilde{\beta}^{\mu} = P\beta^{\mu} - \beta^{\mu}P$. The form for U is

$$U = U_s I + U_s^1 P + \beta^{\mu}U_v + \beta^{\mu}PU_v^1. \tag{4}$$

The last two terms may also be written as $\beta^{\mu}U_v + P\beta^{\mu}U_v^1$.

In order to construct impulse approximation optical potentials consistent with Eq. (4) we need an invariant form for the meson-nucleon t-matrix. The choice for the invariant form used here is

$$t = I_N I t_s + I_N P t_s^1 + \gamma_\mu \beta^\mu t_v + \gamma_\mu \beta^\mu P t_v^1, \tag{5}$$

where I_N and γ_μ are the unit and Dirac γ-matrices for the nucleon. As in the nucleon-nucleus RIA we equate the matrix elements of the empirical c.m. scattering amplitude,

$$F(q) = \hat{f}(q) + \vec{\sigma} \cdot \vec{n} \hat{g}(q), \tag{6}$$

taken between Pauli spinors for the nucleon with the matrix elements of the invariant t-matrix between Dirac and Kemmer free particle spinors. The scattering amplitude and the invariant t-matrix are related by a (2×4) matrix. In this work we limit the t-matrix to only two of the four possible terms in Eq. (5). Thus, we consider models with two scalars, two vectors or a vector-scalar mixture. For each choice a transformation matrix K relates t and F. For example, for a scalar-vector mixture

$$\begin{pmatrix} t_s \\ t_v \end{pmatrix} = -\frac{2\pi\sqrt{s}\, K^{-1}}{Mm} \begin{pmatrix} \hat{f} \\ \hat{g} \end{pmatrix}, \tag{7}$$

where $\sqrt{s}$ is the total meson-nucleon energy and $m(M)$ is the meson (nucleon) mass.

The combination of two scalars or two vectors produces a matrix K with zero determinant, thus, we consider t to consist of a scalar and a vector amplitude. There are, however, several choices for the form of t depending on whether the operator P is in both terms (case 1), in the scalar only (case 2), in the vector only (case 3) or in neither (case 4). The forms $\gamma_\mu P \beta^\mu t_v^1$ and $\gamma_\mu \beta^\mu P t_v^1$ produce identical results. The elements of K for case 1 are given by

$$K_{11}^1 = \frac{1}{4M(E+M)} \left[(E+M)^2 - k^2 + \frac{1}{4} q^2 \right], \tag{8}$$

$$K_{12}^1 = \frac{1}{4M(E+M)} \left(\frac{E_m}{m} \right) \left[(E+M)^2 + k^2 - \frac{1}{4} q^2 \right] + \frac{k^2}{2mM}, \tag{9}$$

$$K_{21}^1 = \frac{ikq}{4M(E+M)}, \tag{10}$$

and

$$K_{22}^1 = \frac{-ikq}{4M(E+M)} \left(\frac{E_m}{m} \right) - \frac{ikq}{4mM}, \tag{11}$$

where $E(E_m)$ is the c.m. energy of the nucleon (meson), $q = 2K \sin\theta/2$ and $k = K \cos\theta/2$, where θ is the c.m. scattering angle and K is the c.m. momentum. For case 2: $K_{11}^2 = K_{11}^1$, $K_{12}^2 = 2K_{12}^1$, $K_{21}^2 = K_{21}^1$ and $K_{22}^2 = 2K_{22}^1$. For case 3: $K_{11}^3 = 2cK_{11}^1$, $K_{12}^3 = K_{12}^1$, $K_{21}^3 = 2cK_{21}^1$ and $K_{22}^3 = K_{22}^1$ where $c = \left(1 + \frac{q^2}{4m^2}\right)$. For case 4: $K_{11}^4 = K_{11}^3$, $K_{12}^4 = 2K_{12}^1$, $K_{21}^4 = K_{21}^3$ and $K_{22}^4 = 2K_{22}^1$. Note that t_s and t_v depend on both $\hat{f}$ and $\hat{g}$, thus, even in the impulse approximation, the scalar and vector potentials contain contributions from $\hat{f}$ and $\hat{g}$. The usual first-order nonrelativistic calculation only contains contributions from $\hat{f}$, see Ref. 20).

The invariant amplitudes for each of the four cases are used to construct optical potentials for use in Eq. (3). The optical potentials for spin zero targets are given by

$$U_{s,v} = \sum_{i=p,n} \int \frac{dq^3}{(2\pi)^3} e^{i\vec{q}\cdot\vec{r}} t^i_{s,v}(q) \rho^i_{s,v}(q), \tag{12}$$

where $\rho_{s,v}(q)$ are the Fourier transforms of the relativistic Hartree densities of Furnstahl et al.[16] The KDP equation for meson-nucleus scattering may now be written as

$$[i\beta^\mu \partial_\mu - A_\mu \beta^\mu - U_j - m]\phi = 0, \tag{13}$$

where $j = 1, 2, 3, 4$ for the four cases used and the electromagnetic potential A_μ has been added by minimal substitution. We take A_μ as the static Coulomb potential obtained from the empirical charge distribution. In addition, the space-like components of U_v do not contribute for spin zero targets.[21]

The KDP elastic cross sections are obtained by solving the second-order equation obtained for the first component of the KDP wave function. For conserved vector current interactions, such as the EM interaction, this second-order equation is identical to the KG equation for EM interactions. Here, however, a different second-order equation results for each case. They are:

$$\text{Case 1: } [(E - U_c - U_v)(E - U_c) - m(m + U_s) + \nabla^2]\phi_1 = 0; \tag{14}$$

$$\text{Case 2: } [(E - U_c - U_v)^2 - m(m + U_s) + \nabla^2]\phi_1 = 0; \tag{15}$$

$$\text{Case 3: } [(E - U_c - U_v)(E - U_c) - (m + U_s)^2 + \nabla^2 - \vec{U}_D \cdot \vec{\nabla}]\phi_1 = 0; \tag{16}$$

$$\text{Case 4: } [(E - U_c - U_v)^2 - (m + U_s)^2 + \nabla^2 - \vec{U}_D \cdot \vec{\nabla}]\phi_1 = 0; \tag{17}$$

where

$$\vec{U}_D = \frac{1}{m + U_s} \vec{\nabla} U_s \tag{18}$$

and U_c is the static Coulomb potential. The non-local Darwin term may be replaced by an equivalent local term using a wave function transformation, just as in the second-order Dirac equation.[21]

It is possible to write Eqs. (14)–(17) as

$$\left\{ \frac{1}{2E} \left[\nabla^2 + U_c^2 - 2EU_c + E^2 - m^2 \right] - U \right\} \phi_1 = 0, \tag{19}$$

which allows us to define an effective central potential U. These complex optical potentials arise from cancellation between large scalar and vector terms, just as in the nucleon-nucleus RIA. We find that the kaon effective potentials resemble the nuclear densities.

In Ref. 3) it was shown that all four choices for the $K^+ + A$ optical potentials produced essentially identical differential cross section predictions for 800 MeV/c K^+ + ^{40}Ca elastic scattering. The Case 1 potential, which yields the best results for $\pi^\pm + A$ elastic scattering,[3] was used in the calculations presented here.

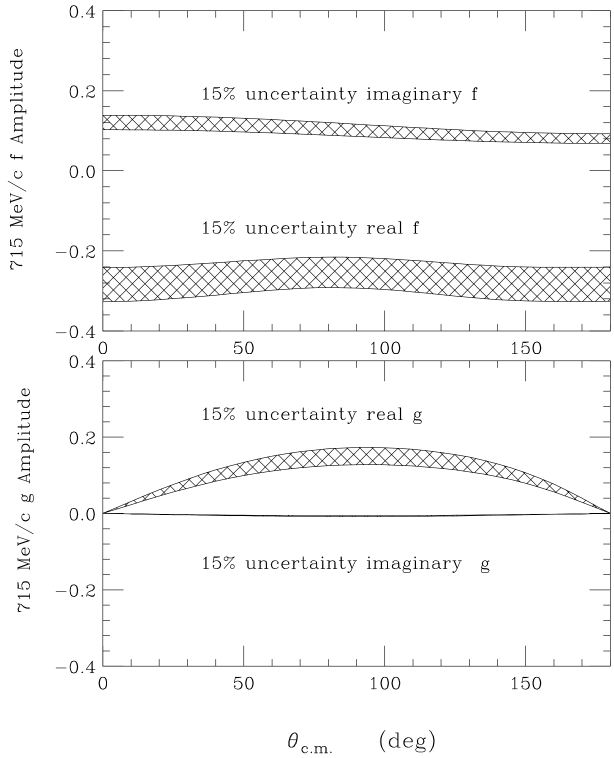

Fig. 1. The real and imaginary elementary amplitudes at 715 MeV/c as a function of center of mass angle.

The imaginary part of the K^+N spin-dependent amplitude $\hat{g}$ is essentially zero for all angles at the energies considered in this work and the real part of $\hat{g}$ is small at the forward angles. Because of this one would expect KDP and the simplest nonrelativistic impulse approximation calculation, which only includes $\hat{f}$, to be quite similar. This is the case as shown in Refs. 3) and 21). In Fig. 1 we show the real and imaginary $\hat{f}$ and $\hat{g}$ K^+N amplitudes at 715 MeV/c as a function of the center of mass angle.

§3. Deducing total and reaction cross sections from transmission data

Total cross section experiments such as those of Refs. 7), 8) and 13) use transmission arrays which consist of a series of thin cylindrical counters of increasing radii whose axes coincide with the beam axis. Thus, measurements summing the $\geq i^{\rm th}$ counters determine a transmission cross section $\sigma_{\rm Trans}(\Omega_i)$ for scattering out of a solid angle Ω_i. For uncharged particles $\sigma_{\rm Trans}(\Omega_i)$ is a well-behaved function near $\Omega_i = 0$, and the total cross section is found by measuring $\sigma_{\rm Trans}(\Omega_i)$ for several values of Ω_i near zero and then extrapolating $\sigma_{\rm Trans}(\Omega_i)$ to $\Omega_i = 0$.

For K^+ or other charged particles, $\sigma_{\rm Trans}(\Omega_i)$ is not well-behaved near $\Omega_i = 0$ since the Coulomb interaction leads to an infinite total cross section. However, a finite total nuclear cross section ($\sigma_{\rm Tot}$) can be determined if Coulomb effects are removed. Thus, for each measured transmission cross section, appropriate Coulomb correction terms are subtracted. The corrected partial cross sections are then fit to a polynomial in Ω_i and, by extrapolating the fit to $\Omega_i = 0$, the finite quantity $\sigma_{\rm Ext}$ is determined:

$$\sigma_{\rm Ext} = \lim_{\Omega_i \to 0} \left[\sigma_{\rm Trans}(\Omega_i) - \text{calculated corrections}\right]. \tag{20}$$

The final value of the total cross section, $\sigma_{\rm Tot}$, is given by

$$\sigma_{\rm Tot} = \sigma_{\rm Ext} - \sigma_K - \sigma_{\pi\text{-}\mu} - \sigma_{\rm A^t}, \tag{21}$$

where σ_K and $\sigma_{\pi\text{-}\mu}$ correct for kaons which decay between the target and detector and for the pion and muon contamination from these decays, and the $\sigma_{\rm A^t}$ term corrects for target impurities.[7),8)] While Eq. (21) concerns experimental corrections, some model of the $K^+ + A$ interaction must be used to calculate the correction terms in Eq. (20). Thus, $\sigma_{\rm Ext}$ and $\sigma_{\rm Tot}$ are model-dependent quantities. We emphasize that at a minimum, when comparing experimental and theoretical total cross sections, the *same* model should be used to calculate the theoretical total cross sections as is used to calculate the correction terms used to remove Coulomb effects. If different optical models are used for the extraction of the experimental total cross sections and the theoretical total cross sections the comparison is flawed. This point has been made in the work of Friedman et al.,[13)] see for example their figure 1 which clearly shows the importance of using the same optical potential in obtaining the extrapolated cross section and the comparison with theory.

The necessary correction terms are found using the method of Ref. 22). The $K^+ + A$ scattering amplitude f, found using an optical model for the interaction as described in the preceding section, is split into a Coulomb distorted nuclear part, f_N, and a Coulomb part, f_C, by adding and subtracting the Coulomb amplitude,

$$\begin{aligned} f &= (f - f_C) \; + \; f_C \\ &= f_N \; + \; f_C, \end{aligned} \tag{22}$$

where the Coulomb distorted nuclear amplitude (f_N) is defined in the last equation. The elastic differential cross section is written as the sum of three terms:

$$\frac{d\sigma}{d\Omega} = |f|^2 = |f_N|^2 + |f_C|^2 + 2{\rm Re}\, f_N f_C^*. \tag{23}$$

The following quantities are defined for a given solid angle Ω_i:

$$\sigma_C(>\Omega_i) = \int_{\Omega_i}^{4\pi} d\Omega |f_C|^2, \tag{24a}$$

$$\sigma_{CN}(>\Omega_i) = 2{\rm Re} \int_{\Omega_i}^{4\pi} d\Omega f_N f_C^*, \tag{24b}$$

$$\sigma_e(<\Omega_i) = \int_0^{\Omega_i} d\Omega |f_N|^2. \tag{24c}$$

Using these definitions, Eq. (20) becomes

$$\sigma_{\rm Ext} = \lim_{\Omega_i \to 0} \left[\sigma_{\rm Trans}(\Omega_i) - \sigma_C(>\Omega_i) - \sigma_{CN}(>\Omega_i) + \sigma_e(<\Omega_i) + \sigma_I(<\Omega_i) \right], \quad (25)$$

where the inelastic term $\sigma_I(<\Omega_i)$, assumed to be small, is neglected in obtaining the limit. For this model, the theoretical total cross section is found by using a partial wave expansion of the scattering amplitude. The expression is given in Eq. (20) of Ref. 22).

Determination of the reaction cross section follows a similar procedure. As outlined in Ref. 13), the reaction cross section is defined to be the integral cross section for removal of particles from the elastic channel. In terms of the measured transmission cross sections for scattering out of a solid angle Ω,

$$\sigma_{\rm Trans}(\Omega) = \sigma_{\rm Reac} + \int_{\Omega}^{4\pi} d\Omega \left(\frac{d\sigma}{d\Omega} \right)_{\rm elastic} - \int_0^{\Omega} d\Omega \left(\frac{d\sigma}{d\Omega} \right)_{\rm inelastic}. \quad (26)$$

Since the small, inelastic term vanishes as $\Omega \to 0$, the experimental total reaction cross section is found by extrapolating the quantity

$$\sigma_{\rm Reac}(\Omega) \equiv \sigma_{\rm Trans}(\Omega) - \int_{\Omega}^{4\pi} d\Omega \left(\frac{d\sigma}{d\Omega} \right)_{\rm elastic} \quad (27)$$

to $\Omega = 0$ and subtracting the σ_K, $\sigma_{\pi\text{-}\mu}$ and $\sigma_{\rm A^t}$ experimental corrections.

§4. Results and discussion

The KDP-RIA model was used to calculate scattering observables for 450 – 750 MeV/c K^+ + ^{6}Li, ^{12}C, ^{28}Si and ^{40}Ca. The same model was then used to extract experimental $\sigma_{\rm Tot}$ and $\sigma_{\rm Reac}$ from transmission data [7), 8), 13)] spanning 488 – 714 MeV/c. Figures 2–5 show (solid circles) the experimental $\sigma_{\rm Tot}$ and $\sigma_{\rm Reac}$ cross sections obtained here. Also shown in Figs. 2–5 (solid squares) are experimental values which we obtained from the transmission data [7), 8), 13)] using model-dependent corrections derived from solution of the Schrödinger equation with relativistic kinematics and the "$t\rho$" optical potential from Ref. 13). The error bars are statistical only. Our "$t\rho$" cross sections are consistent with those in Table II of Ref. 13). As seen from Figs. 2–5, the model-dependences in the experimental cross sections are, in general, larger than the statistical errors and are greater for $\sigma_{\rm Tot}$ than for $\sigma_{\rm Reac}$. We consider this to be significant because the model dependence is larger in magnitude than the statistical errors in the extracted experimental total cross sections.

In Table I we compare the results of the present work (last row) for experimental $\sigma_{\rm Reac}$ and $\sigma_{\rm Tot}$ with those (first and second rows) taken from Table IV of Ref. 13). The $t\rho$ potential of Ref. 13) is proportional to the product of the forward K^+N spin-independent scattering amplitude $[\hat{f}_{K^+N}(0)]$ and the nuclear density $\rho(r)$, while the *DD* potential of Ref. 13) is an *ad hoc* phenomenological density-dependent modification of the interaction to constrain the analysis to fit elastic scattering data. The *DD*-$t\rho$ comparison shows that the experimental $\sigma_{\rm Reac}$ is not sensitive to the choice of potential, while the same cannot be said for $\sigma_{\rm Tot}$, where the differences span 5 – 11%.

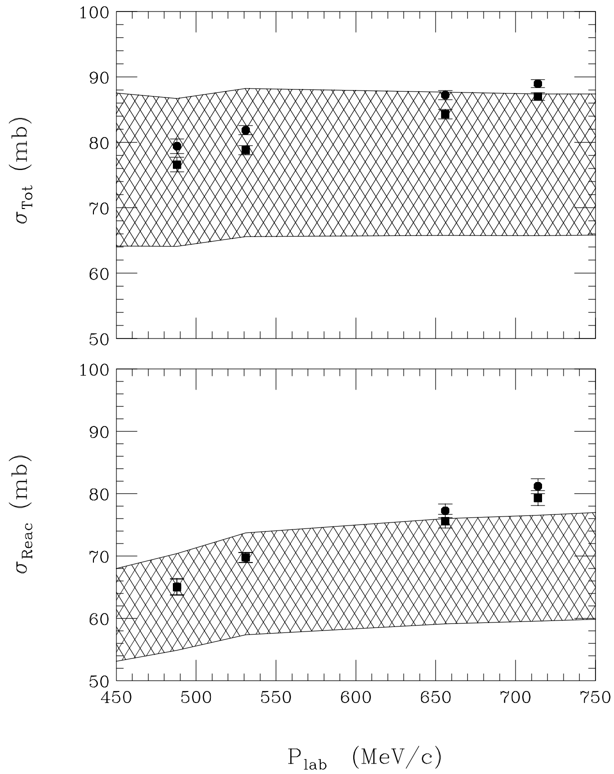

Fig. 2. The experimental and theoretical total cross sections and reaction cross sections for K^++^{6}Li as a function of incident laboratory momentum. The experimental values obtained using the KDP-RIA relativistic optical model calculated corrections are shown as solid circles and those obtained using the "$t\rho$" optical model of Ref. 13) are shown as solid squares. The theoretical total and reaction cross section results are plotted as a band of values which take into account the uncertainties in the elementary K^+N amplitudes used in the calculation.

Table I. $K^+ + A$ total and reaction cross sections extracted from 714 MeV/c transmission data using three different models for the extrapolations.

	Reaction (mb)				Total (mb)			
Potential	^{6}Li	^{12}C	^{28}Si	^{40}Ca	^{6}Li	^{12}C	^{28}Si	^{40}Ca
DD a)	80.0	149.2	317.7	413.4	91.2	192.1	433.9	589.6
$t\rho$ a)	79.3	149.3	317.5	412.9	87.0	175.6	396.5	528.4
$t_{\rm eff}\rho$ b)	82.2	152.8	320.2	417.1	88.5	183.8	411.3	550.4
KDP-RIA c)	81.2	151.9	316.9	413.9	88.9	180.4	405.7	547.1

a) From Ref. 13).

b) From Refs. 23) and 24).

c) Using the same extrapolation method as Ref. 13).

In addition, in row three of Table I we include the more recent results of Refs. 23) and 24) which employ an effective t-matrix, $t_{\rm eff}(\rho)$, which is density dependent.

The predicted total and reaction cross sections from the KDP-RIA theoretical model are shown as shaded bands in Figs. 2–5. The bands result from the uncertainties in the elementary K^+N amplitudes.[17] Contributions to the error bands due to

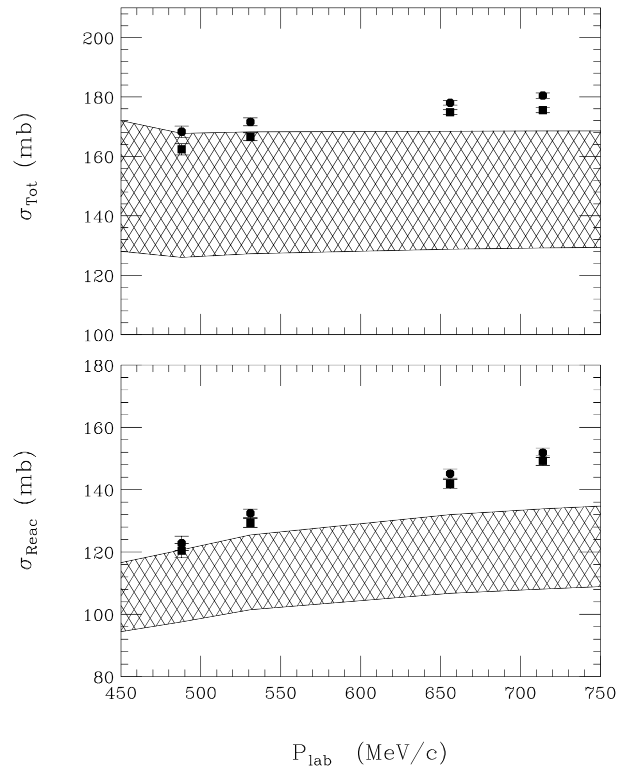

Fig. 3. Same as Fig. 2 except for K^++^{12}C.

uncertainties in the nuclear densities were studied in Ref. 13) and shown to be small and were not included here. Some of the conventional $K^+ + A$ medium corrections have been shown to contribute only a few percent to the first-order impulse approximation predictions (Ref. 13) and references therein) and were not included here. Additional medium corrections (e.g. Pauli blocking and nuclear binding potentials in intermediate K^+N scattering states) and second-order optical potential (correlation) terms also remain to be included. Recent discussions of the status of medium effects in K-A interactions are given in Refs. 13), 23)–25).

For first-order impulse approximation predictions of $K^+ + A$ total and reaction cross sections, the critical components of the input K^+N amplitudes are the forward angle spin-independent terms, $\hat{f}_{K^+N}(0)$. These are determined experimentally by the K^+N total cross sections and the real-to-imaginary forward amplitude ratios. For K^+p the scatter in the measured $\sigma_{\rm Tot}(K^+p)$ [26] in the momentum range from 450 to 750 MeV/c is about ± 1 mb corresponding to an $\sim$8% uncertainty in ${\rm Im}\hat{f}_{K^+p}(0)$. The uncertainty in ${\rm Re}\hat{f}_{K^+p}(0)$ is about 20%.[17] However, for K^+n there are no direct measurements for either of these quantities. The K^+n total cross section is estimated from the difference between the total cross sections for K^+d and K^+p plus some theoretical rescattering and deuteron structure corrections.[15),27)] The uncertainty in ${\rm Im}\hat{f}_{K^+n}(0)$ is therefore larger than that for K^+p. The ${\rm Re}\hat{f}_{K^+n}(0)$ is estimated from dispersion relation calculations [15),28),29)] and is about 50% uncertain.

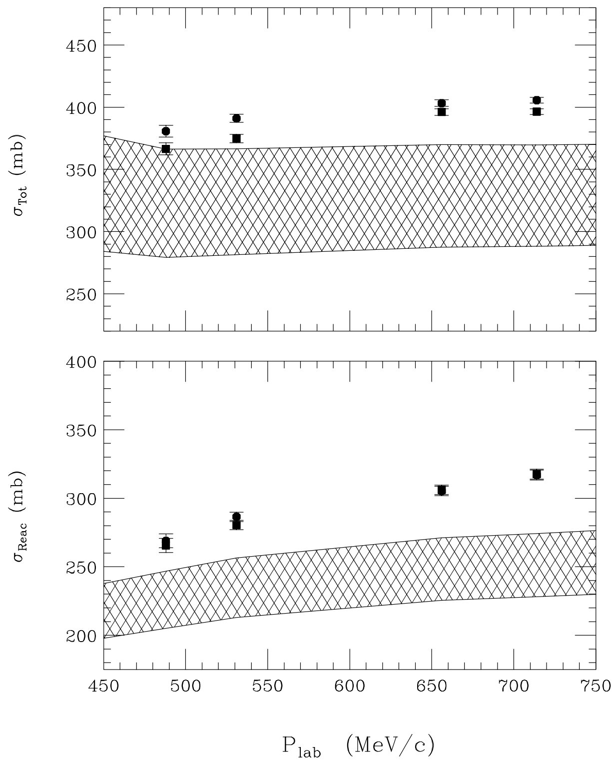

Fig. 4. Same as Fig. 2 except for $K^+ + {}^{28}$Si.

The uncertainties vary with amplitude and angle; an overall estimate of the global error, relevant for these calculations, is $\pm 15\%$.[17] This is what we use to calculate the error due to the uncertainty in the amplitudes (see Fig. 1). We note that in contrast to Refs. 13), 23)–25) we use angle dependent K^+N amplitudes in obtaining the KDP-RIA optical potentials.

Previous authors have studied total cross section ratios for K^+A/K^+d in order to minimize the errors due to the uncertainties in the K^+N amplitudes. However, the theoretical model appropriate for K^+A scattering (e.g. optical potential) is very different from that which is best suited for K^+d scattering (e.g. multiple scattering expansion[30]). The cancellation of theoretical uncertainties for the K^+A and K^+d predictions is therefore problematic. Since the theoretical predictions for $\sigma_{\rm Tot}(K^+d)$ cannot be tested or "calibrated" to any greater accuracy than that allowed by the uncertainties in the K^+N amplitudes, the latter source of uncertainty continues to contribute, in effect, to the predicted cross section ratios. In this work we choose to compare our $K^+ + A$ scattering predictions directly with the $K^+ + A$ scattering data.

In Fig. 1 of Ref. 13) the optical model contributions to $\sigma_{\rm Reac}$ are shown to be less than that for $\sigma_{\rm Tot}$ and to vanish as Ω increases. This suggests that $\sigma_{\rm Reac}$ is the more reliable quantity (i.e., less model-dependent) that may be derived from transmission measurements. In viewing the uncertainty bands in Figs. 2–5, it is seen that the

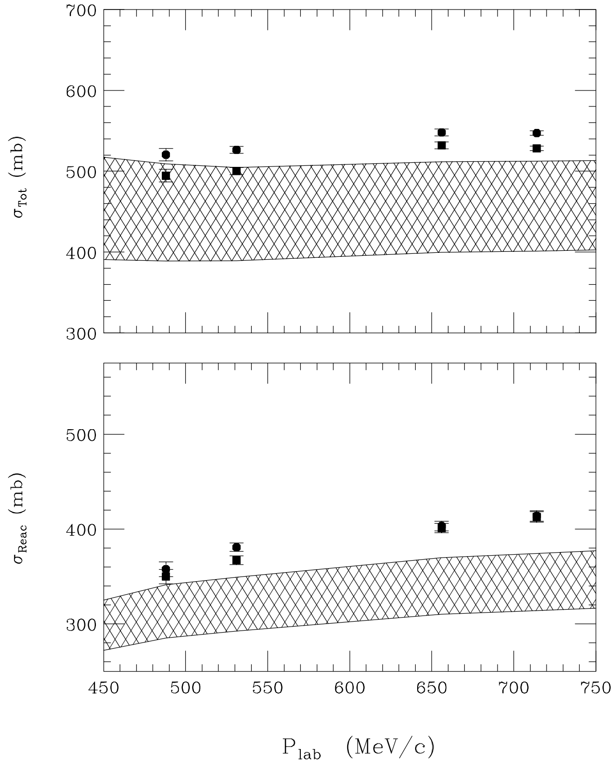

Fig. 5. Same as Fig. 2 except for K^++^{40}Ca.

predicted reaction cross sections are also less sensitive to uncertainties in the input. Given the uncertainties in the theoretical predictions, the agreement with the ^{6}Li data is reasonable, whereas the predictions for the heavier targets are systematically smaller than the data, and may suggest that some additional dynamics in the K^+-nucleus interaction remains to be taken into account. However, the mass-dependence may also indicate a still unrealized experimental problem associated with Coulomb scattering corrections owing to the strong Z^2-dependence of Coulomb scattering.

In Fig. 6 the KDP-RIA prediction for the 715 MeV/c K^++^{12}C elastic differential cross section is compared with the data of Ref. 12). The shaded band indicates the uncertainty due to that in the K^+N amplitudes. The agreement with the data is good, but the shaded error band in this figure, as well as those in Figs. 2–5, suggests that the elementary K^+N amplitudes need to be better determined if progress and further theoretical understanding of these data are going to be made. The present situation is similar to that encountered during the early days of medium energy $p+A$ studies [31)] when the elementary $p+N$ amplitudes were not sufficiently well-determined at the momentum transfers important for generating $p+A$ optical potentials.

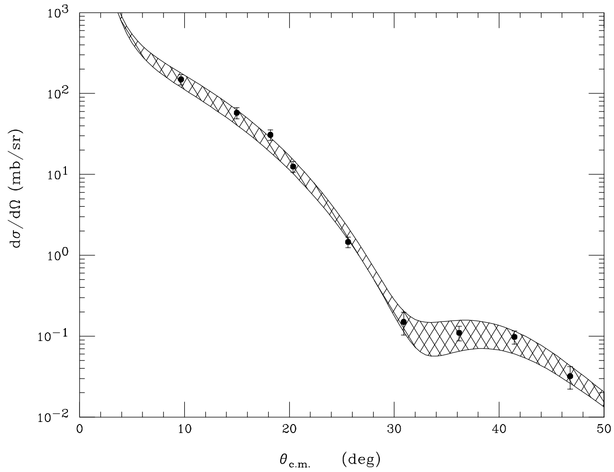

Fig. 6. The experimental and theoretical elastic differential cross sections for 715 MeV/c K^++^{12}C as a function of center of mass angle. The results obtained using the KDP-RIA relativistic optical model are plotted as a band of values which take into account the uncertainties in the elementary K^+N amplitudes.

§5. Conclusions

The relativistic KDP-RIA meson-nucleus scattering model was applied to medium energy $K^+ + A$ elastic scattering and predictions for the total cross section, total reaction cross section, and differential cross section were compared with experiment. The KDP-RIA total and reaction cross section predictions are consistent with the $K^+ + {}^6$Li data but systematically underpredict the $K^+ + {}^{12}$C, ^{28}Si and ^{40}Ca data. The 715 MeV/c $K^+ + {}^{12}$C differential cross section predictions are in quantitative agreement with experiment. Overall, the KDP-RIA framework provides a reliable model for relating the K^+N amplitude phenomenology and nuclear densities to the $K^+ + A$ elastic scattering observables. However, this alternate reaction model does not resolve the kaon-nucleus total cross section issues described in the introduction.

The model dependence in the total and reaction cross sections deduced from the transmission measurements was studied and found to be larger than the statistical errors for $\sigma_{\rm Tot}$. The model dependence in the extracted values for $\sigma_{\rm Tot}$ was found to be of order 5 – 11%, which is significant but does not explain the discrepancy between the predictions and the data. The model dependence for $\sigma_{\rm Reac}$ is much less, being only 1 – 3%. Consistent comparisons between theoretical and "experimental" total and reaction cross sections require that the same $K^+ + A$ scattering model be used in both analyses. To enable consistent analyses by others in the community, the transmission cross section data should be included in publications which present total and reaction cross sections extracted from such data.

Uncertainties in the $K^+ + A$ theoretical predictions arising from the uncertainties in the K^+N amplitudes were estimated for the total and reaction cross sections and the 715 MeV/c $K^+ + {}^{12}$C elastic differential cross section. Uncertainties of order ±13% (±10%) were obtained for the $K^+ + A$ $\sigma_{\rm Tot}$ ($\sigma_{\rm Reac}$) predictions. Part of the longstanding discrepancy between theoretical $K^+ + A$ total and reaction cross section predictions and experiment might therefore be due to inaccuracies in the input K^+N amplitudes. In our opinion, improved knowledge of the K^+N amplitudes is required before studies of additional K^+- nucleus dynamical effects can be meaningfully pursued.

Acknowledgements

The authors thank E. D. Cooper, for his many contributions to this work. The authors also thank J. Alster, R. Chrien, E. Friedman, K. H. Hicks, E. V. Hungerford, E. Piasetzky, R. Sawfta and R. Wiess for helpful discussions and information regarding the experimental aspects of $K^+ + A$ total cross section analysis and for providing information needed to calculate the optical model dependent corrections to σ_{Ext}. B. C. Clark, L. Kurth Kerr and S. Hama acknowledge the hospitality of the National Institute for Nuclear Theory, University of Washington where part of this work was done. This work was supported in part by NSF PHY-9511923, NSF PHY-9800964, the U. S. Department of Energy Grant DE-FG03-94ER40845, and the Robert A. Welch Foundation Grant F-604.

References

1) W. R. Coker, G. W. Hoffmann and L. Ray, Phys. Lett. **135B** (1985), 363.
2) D. Marlow, P. D. Barnes, N. J. Colella, S. A. Dytman, R. A. Eisenstein, R. Grace, F. Takeutchi, W. R. Wharton, S. Bart, D. Hancock, R. Hackenberg, E. Hungerford, W. Mayes, L. Pinsky, T. Williams, R. Chrien, H. Palevsky and R. Sutter, Phys. Rev. **C25** (1982), 2619.
3) B. C. Clark, S. Hama, G. R. Kälbermann, R. L. Mercer and L. Ray, Phys. Rev. Lett. **55** (1985), 592 and references therein.
4) P. B. Siegel, W. B. Kaufmann and W. R. Gibbs, Phys. Rev. **C31** (1985), 2184.
5) C. M. Chen and D. J. Ernst, Phys. Rev. **C45** (1992), 2019.
6) M. F. Jiang, D. J. Ernst and C. M. Chen, Phys. Rev. **C51** (1995), 857.
7) R. Weiss, J. Aclander, J. Alster, M. Barakat, S. Bart, R. E. Chrien, R. A. Krauss, K. Johnston, I. Mardor, Y. Mardor, S. May Tal-beck, E. Piasetzky, P. H. Pile, R. Sawafta, H. Seyfarth, R. L. Stearns, R. J. Sutter and A. I. Yavin, Phys. Rev. **C49** (1994), 2569.
8) R. A. Krauss, J. Alster, D. Ashery, S. Bart, R. E. Chrien, J. C. Hiebert, R. R. Johnson, T. Kishimoto, I. Mardor, Y. Mardor, M. A. Moinester, R. Olshevsky, E. Piasetzky, P. H. Pile, R. Sawafta, R. L. Stearns, R. J. Sutter, R. Weiss and A. I. Yavin, Phys. Rev. **C46** (1992), 655.
9) P. B. Siegel, W. B. Kaufmann and W. R. Gibbs, Phys. Rev. **C30** (1984), 1256.
10) G. E. Brown, C. B. Dover, P. B. Siegel and W. Weise, Phys. Rev. Lett. **60** (1988), 2723.
11) J. C. Caillon and J. Labarsouque, Phys. Rev. **C45** (1992), 2503.
12) R. Michael, M. B. Barakat, S. Bart, R. E. Chrien, B. C. Clark, D. J. Ernst, S. Hama, K. H. Hicks, E. V. Hungerford, M. F. Jiang, T. Kishimoto, C. M. Kormanyos, L. J. Kurth, L. Lee, B. Mayes, R. J. Peterson, L. Pinsky, R. Sawafta, R. Sutter, L. Tang and J. E. Wise, Phys. Lett. **B382** (1996), 29.
13) E. Friedman, A. Gal, R. Weiss, J. Aclander, J. Alster, I. Mardor, Y. Mardor, S. May-Tal Beck, E. Piasetzky, A. I. Yavin, S. Bart, R. E. Chrien, P. H. Pile, R. Sawafta, R. J. Sutter, M. Barakat, K. Johnston, R. A. Krauss, H. Seyfarth and R. L. Stearns, Phys. Rev. **C55** (1997), 1304.
14) B. C. Clark, S. Hama, R. L. Mercer, L. Ray and B. D. Serot, Phys. Rev. Lett. **50** (1983), 1644.
15) R. A. Arndt and L. D. Roper, Phys. Rev. **D31** (1985), 2230.
J. S. Hyslop, R. A. Arndt, L. D. Roper and R. L. Workman, Phys. Rev. **D46** (1992), 961.

16) R. J. Furnstahl, C. E. Price and G. W. Walker, Phys. Rev. **C36** (1987), 2590.
17) R. A. Arndt, interactive computer code and data base SAID and private communication. Percentage errors are given for Single-Energy solutions only, and vary strongly with amplitude and angle. 15% is an overall estimate for the global error.
18) E. Fishbach, M. M. Nieto and C. E. Scott, J. Math. Phys. **14** (1973), 1760; Phys. Rev. **D7** (1973), 207.
19) R. F. Guertin and T. L. Wilson Phys. Rev. **D15** (1977), 1518.
20) W. R. Coker, J. D. Lumpe and L. Ray, Phys. Rev. **C31** (1985), 1412.
21) B. C. Clark, in *Relativistic Dynamics and Quark-Nuclear Physics*, ed. Mikkel B. Johnson and Alan Picklesimer (Wiley-Interscience Publication, 1986), p. 302.
22) W. B. Kaufmann and W. R. Gibbs, Phys. Rev. **C40** (1989), 1729.
23) E. Friedman, A. Gal and J. Mareš, Phys. Lett. **B396** (1997), 21.
24) E. Friedman, A. Gal and J. Mareš, Nucl. Phys. **A625** (1997), 272.
25) A. Gal, Nucl. Phys. **A639** (1998), 485c.
26) J. J. Hernandez et al. (Particle Data Group), Phys. Lett. **B239** (1990), p. III.80.
27) A. S. Carroll, T. F. Kycia, K. K. Li, D. N. Michael, P. M. Mockett, D. C. Rahm and R. Rubinstein, Phys. Lett. **B45** (1973), 531.
28) K. Hashimoto, Phys. Rev. **C29** (1984), 1377.
29) B. R. Martin, Nucl. Phys. **B94** (1975), 413.
30) G. Alberi, M. Bleszynski and T. Jaroszewicz, Ann. of Phys. **142** (1982), 299.
31) L. Ray, Phys. Rev. **C19** (1979), 1855.